CHEMMEDCHEM

CHEMISTRY ENABLING DRUG DISCOVERY

Accepted Article

Title: Switchable fluorescence of doxorubicin for label-free imaging of bioorthogonal drug release

Authors: Taha Bilal Uyar, Kui Wu, Muhan He, Irfan Khan, Maksim Royzen, and Mehmet V. Yigit

To be cited as: *ChemMedChem* 10.1002/cmdc.202000065

Link to VoR: http://dx.doi.org/10.1002/cmdc.202000065

A Journal of

ChemPubSoc Europe

WILEY-VCH

www.chemmedchem.org

WILEY-VCH

FULL PAPER

Switchable fluorescence of doxorubicin for label-free imaging of bioorthogonal drug release

Taha Bilal Uyar,[a] Kui Wu,[a] Muhan He,[a] Irfan Khan,[a] Maksim Royzen,*[a, b] and Mehmet V. Yigit*[a, b]

[a] Dr. T. B. Uyar, Dr. K. Wu, M. He, Dr. I. Khan, Prof. M. Royzen and Prof. M. V. Yigit
Department of Chemistry,
University at Albany, State University of New York,
1400 Washington Avenue, Albany, New York 12222, United States.
Email: myigit@albany.edu and mroyzen@albany.edu

[b] Prof. M. V. Yigit and Prof. M. Royzen

The RNA Institute,
University at Albany, State University of New York,
1400 Washington Avenue, Albany, New York 12222, United States.
Email: myigit@albany.edu and mroyzen@albany.edu

Supporting information for this article is given via a link at the end of the document.

Abstract: Monitoring the release and activation of prodrug formulations provides essential information about the outcome of a therapy. While the prodrug delivery can be confirmed using different imaging techniques, confirming the release of active payload using imaging is a challenge. Here, we have discovered that the switchable fluorescence of doxorubicin can validate drug release upon its uncaging reaction with a highly specific chemical partner. We have observed that the conjugation of doxorubicin with a *trans*-cyclooctene diminishes its fluorescence at 595 nm. This quenched fluorescence of doxorubicin prodrug is recovered upon its bond-cleaving reaction with tetrazine. Clinically assessed iron oxide nanoparticles were used to formulate a doxorubicin nanodrug. The release of doxorubicin from nanodrug was studied under various experimental conditions. Five-fold increase in doxorubicin fluorescence is observed after complete release. The studies were carried out *in vitro* using MDA-MB-231 breast cancer cells. Increase in Dox signal was observed upon tetrazine administration. This switchable fluorescence mechanism of Dox could be employed for fundamental studies, i.e., the reactivity of various tetrazine and TCO linker types under different experimental conditions. In addition, the system could be instrumental for translational research where the release and activation of doxorubicin prodrug payloads can be monitored using optical imaging systems.

Introduction

Spatiotemporal delivery and activation of prodrug formulations are essential for an effective battle against human diseases, particularly against cancer. Extensive efforts have been made for development of alternative drug administration approaches superior to the conventional methods.[1] Since the potential of nanoparticles for *in vivo* delivery is undeniable, substantial efforts have been demonstrated to translate nanoparticle-drug (nanodrug) formulations into clinic.[2]

The most common nanodrug formulations include attachment of drugs on nanoparticle surface which releases the payload in response to the change in the biochemical environment of the disease sites.[3] Though this approach has been shown to be powerful, the lack of control over drug release is concerning. Some of the challenges include, but not limited to, undesired release of drug payloads in the circulation due to metabolites or variations in the microenvironment of different tissues. Premature drug release could have several unfavorable consequences: (1) loss of valuable drug payload in circulation before its arrival to the target tissue, (2) increase in off-target or side effects and, (3) misleading information about the delivery of nanodrugs to the target tissue. We have recently employed a biocompatible chemistry to address these challenges using several nanodrug formulations.[4]

The drug payloads in these designs were loaded on dextran coated super paramagnetic nanoparticle (NP) surface through *trans*-cyclooctene (TCO) linkers that attenuated the payload's therapeutic function through surface immobilization and chemical derivatization.[4] Once the delivery of the nanodrugs was confirmed, the drug payloads were released upon reaction with a chemical partner, tetrazine, through bond-breaking bioorthogonal chemistry. Our approach offered an operator-controlled drug activation independent of metabolism of the living systems.

One of the overlooked issues in nanodrug formulations is confirmation of the payload release in the target tissues. Often the delivery of the nanodrug is confirmed by exploiting the imaging properties of nanoparticles.[5] For instance, drug-loaded super paramagnetic nanoparticles are imaged by MRI which confirms the delivery of the nanodrug formulations[6] or, fluorescently labeled nanodrugs can be tracked by optical imaging systems to validate the nanodrug circulation.[7] However, it is a challenge to confirm the release and activation of many prodrugs upon their arrival to the target tissue. A biomedical imaging modality with such capacity could provide essential information about therapeutic treatment.

Here, we have demonstrated that doxorubicin's fluorescence is attenuated upon conjugation to TCO and NPs. Doxorubicin (Dox) is a chemotherapeutic drug molecule which has an intrinsic fluorescence peak at 595 nm.[8] The release of doxorubicin from NP surface is accompanied by fluorescence recovery.

Results and Discussion

Dox-TCO-NHS is a small molecule prodrug which is synthesized for the assembly of a Dox nanodrug formulation, **Scheme 1 and S1**. The attached Dox can be released from nanodrug assembly through bond-cleaving bioorthogonal chemistry in response to tetrazine.[4b] We have previously demonstrated that toxicity of Dox-TCO (IC_{50} = 98 nM for Dox-TCO) increases 5-fold after its reaction with tetrazine uncaging unmodified doxorubicin (IC_{50} = 480 nM for Dox).[4c] The Dox is first derivatized with NHS-TCO-NHS which is necessary for its subsequent attachment to NP surface for *click-to-release* studies. This derivatization offers several useful features; i.e., (1) cytoxicity is decreased with TCO modification,[4c] (2) resistance to release in response to endogenous factors and, (3) Dox release specific to its nontoxic chemical partner.[4a, b, 9]

Scheme 1. The fluorescence intensity of Dox decreases after its attachment to TCO. The quenched-fluorescence of Dox-TCO-NHS is recovered upon its bond-cleaving reaction with tetrazine.

Chemical modification of Dox with TCO lowers its fluorescence signal at 595 nm, **Fig. 1b**. The resulting Dox-TCO-NHS prodrug is reactive to tetrazine which is able to recover its fluorescence upon bond-breaking bioorthogonal reaction, **Scheme 1**. First, the NMR and mass spectrometry were used to confirm the synthesis of the Dox-TCO-NHS, **Fig S1 and S2**. The absorbance spectrum of 50 µM of Dox-TCO-NHS was recorded and compared with Dox alone which has an absorbance band between 350-600 nm and a maxima at 484 nm ($\varepsilon_{(484nm)}$ = 11,500 $M^{-1}cm^{-1}$), **Fig 1a**. The derivatization with TCO-NHS shifted absorbance maxima to 493 nm with a 25% decrease in intensity. The extinction coefficient of Dox-TCO-NHS was calculated to be $\varepsilon_{(493nm)}$ = 7,750 $M^{-1}cm^{-1}$, **Fig S3**.

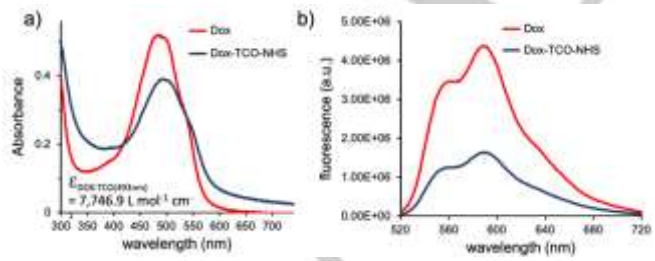

Fig 1. The (a) absorbance and (b) fluorescence spectra of Dox and Dox-TCO-NHS.

Subsequently, the fluorescence spectra of Dox and Dox-TCO-NHS were collected (λ_{ex} = 484 nm) and compared. A sharp decrease in fluorescence at 595 nm was observed after chemical derivatization of Dox with TCO, **Fig. 1b**. We tested whether this change in fluorescence intensity can be reversed upon cleavage of TCO. The Dox-TCO-NHS was reacted with tetrazine and an increase in fluorescence intensity is observed short after the reaction, **Fig 2a**. Thus, a decrease in fluorescence is observed with chemical conjugation of Dox with TCO (Dox → Dox-TCO-NHS) whereas an increase is observed with cleaving reaction with tetrazine (Dox-TCO-NHS → Dox).

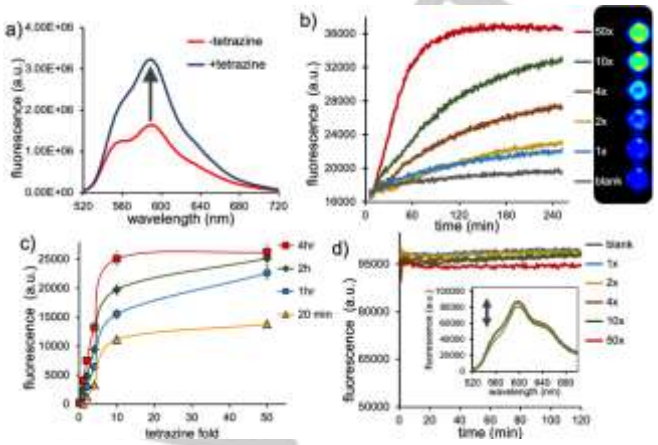

Fig 2. (a) Increase in fluorescence intensity of Dox-TCO-NHS after its reaction with tetrazine. The release kinetics of Dox with (b) various tetrazine concentrations and (c) time points monitored by fluorescence recovery at 595 nm. (b) The fluorescence images 4h post-tetrazine treatment. (d) The fluorescence measurements at 595 nm with different tetrazine concentrations using Dox-TCO-NHS in DMSO.

This switchable fluorescence event could be instrumental for both fundamental and application standpoints. It enables us to study the rate of the bioorthogonal reaction between TCO and tetrazine under different experimental conditions, i.e., pH, time and tetrazine concentrations. On the other hand, the kinetics of Dox release from a solid surface, e.g., nanoparticle; can be recorded in a label-free fashion using optical imaging systems. Reactivity between tetrazine and Dox-TCO-NHS was further investigated using fluorescence.

First, the 10 µM of Dox-TCO-NHS was treated with different amounts of tetrazine over 4 hrs. The rate of the reaction increased dramatically with increased tetrazine concentration, **Fig. 2b**. The final fluorescence of each sample was also recorded using a fluorescence imaging setup and a clear fluorescence recovery is visualized in microplate wells, **Fig. 2b**. It is important the note that the tetrazine itself doesn't display any fluorescence at this experimental wavelength, **Fig. S4**. Later, the change in fluorescence was studied using different time points. Reaction with 50-fold tetrazine administration was complete in about an hour whereas lower tetrazine concentrations required additional time for completion of reaction, **Fig. 2c**. The studies were repeated with 50-fold tetrazine under different acidic conditions to confirm the stability and reactivity of TCO linker at different pHs, **Fig S5**.

Second, we tried to understand the reason why conjugation to TCO causes quenching of Dox fluorescence. Addition of hydrophobic TCO group decreases aqueous solubility of Dox. We hypothesized that the reason for fluorescence quenching could be due to the local aggregation of Dox-TCO-NHS in aqueous media (ACQ).[10] Dox is poorly soluble in water and there have been efforts to increase Dox solubility either by liposomal encapsulation[11] (Doxil: FDA-approved nanodrug delivery system of Dox) or by chemical derivatization for higher dose

administration. In order to test whether ACQ is the reason for the fluorescence-quenching, Dox-TCO-NHS was dissolved in DMSO and treated with different amounts of tetrazine. No fluorescence recovery was observed with any of tetrazine administration, **Fig 2d**. The fluorescence of Dox-TCO-NHS and Dox were measured to be identical in DMSO, (**Fig 2d**-inset**)**. In fact, the fluorescence intensity of Dox-TCO-NHS with/without tetrazine was significantly higher than its fluorescence measured in aqueous solution with same experimental parameters, **Fig 2b and 2d**. The results suggest that the ACQ could be the reason for the reduced fluorescence of Dox-TCO-NHS.

Nevertheless, in order to (1) evaluate whether fluorescence recovery could be observed on a solid support and (2) exploit this property in nanodrug formulations,[12] we have conjugated Dox-TCO-NHS to aminated dextran coated nanoparticles (NPs),[5, 13] **Fig 3a**. The resulting Dox-TCO-NP was subsequently functionalized with cy5.5,[6b] which was used as an internal reference to evaluate qualitative/quantitative Dox release. The absorbance bands of Dox and cy5.5 were observed on the spectrum of Dox-TCO-NP, **Fig 3b**- blue spectrum. The absorbance spectrum of blank NPs was measured (**Fig 3b**- red spectrum**)** and subtracted from that of Dox-TCO-NP to quantify the absorbance intensity (**Fig 3b**- inset) and the number of Dox (75 Dox/NP) and cy5.5 (2.5 cy5.5/NP) per NP.

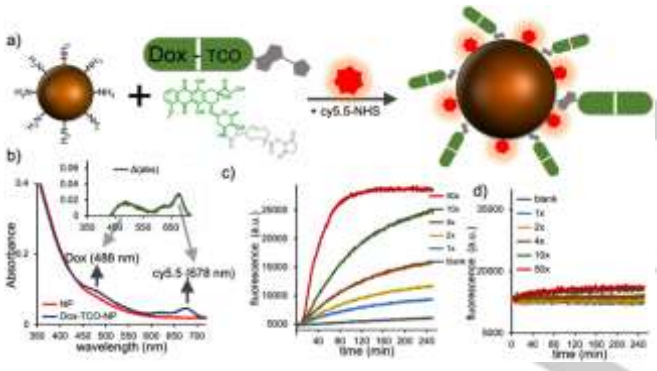

Fig 3. (a) Assembly of Dox-TCO-NP using NPs, Dox-TCO-NHS and cy5.5-NHS. (b) Absorbance spectra of Dox-TCO-NP and NP confirming attachment of both Dox and cy5.5. (c) The release kinetics of Dox from Dox-TCO-NP assembly using various tetrazine amounts measured by fluorescence at 595 nm. (d) No change in cy5.5 fluorescence (700 nm) observed over time under various tetrazine concentrations.

Later the fluorescence recovery of Dox from 150 nM of Dox-TCO-NP formulation was measured using various tetrazine concentrations, **Fig 3c**. The goal was to determine whether fluorescence recovery can be observed upon tetrazine-triggered Dox release, **Fig 4a**. The fluorescence of cy5.5 was measured in parallel (**Fig 3d**) and compared with Dox release. The release kinetics of Dox with different tetrazine concentration suggested that the rate of the recovery increased with tetrazine concentration while cy5.5 signal remained unchanged throughout all readings at different time points and tetrazine amounts.

The tetrazine concentration-dependent release of Dox was quantified using the ratio final fluorescence/initial fluorescence ($\%f/f_0$) readings at the 4h time point. While 5-fold increase in green signal (Dox) is observed with 50-fold tetrazine administration, the red channel (cy5.5, internal reference) remained almost unchanged, **Fig 4b**. The Dox-TCO-NP samples with/without tetrazine administration were imaged at two different fluorescence channels, **Fig 4c**. The overlay of fluorescence images from both channels show a red-to-orange-to-yellow color transition with higher tetrazine concentration indicative of increase in green color with Dox release.

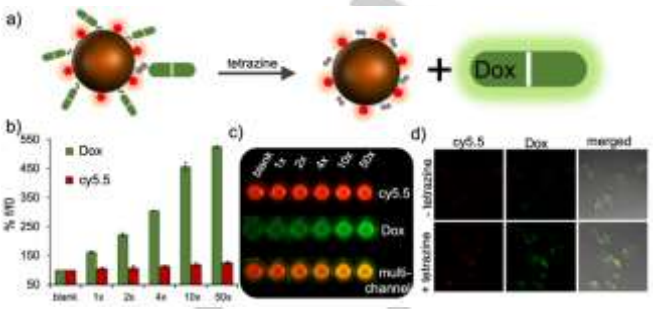

Fig 4. (a) Release of Dox from Dox-TCO-NHS in response to tetrazine result in fluorescence recovery of Dox. (b) Fluorescence recovery (% final fluoresence/initial fluorescnece) of Dox in reference to cy5.5 signal 4 hr after tetrazine administration. Fluroscence images of Dox, cy5.5 and overlayed images in response to (c) different tetrazine concentrations in aqeous solution and (d) *in vitro* (MDA-MB-231) cell environment.

Finally, the Dox release was monitored in live cells using fluorescence imaging, **Fig 4d**. The metastatic MDA-MB-231 breast cancer cells were treated with Dox-TCO-NP followed by tetrazine administration. While the cy5.5 (red) signals were comparable with/without tetrazine administration, the signals from green channel (Dox) were observed to be stronger with tetrazine administration, **Fig 4d**. The overlay of all channels (bright-field, red and green) presents an increase and diffusion of green signal due to release and departure of Dox from the NP surface after tetrazine administration. The flow cytometry (FACS) measurements using cells treated with Dox-TCO-NP indicate increase in fluorescence signal of Dox upon tetrazine administration, **Fig S6**. The fluorescence recovery of Dox-TCO in a model DNA pool is studied using Dox-TCO in M13 dsDNA (~7250-bp long) suspension after tetrazine administration, **Fig S7**.

Conclusion

In conclusion, we have discovered that conjugation of TCO diminishes Dox's intrinsic fluorescence at 595 nm. This quenched fluorescence can be recovered by uncaging of Dox using bioorthogonal bond-cleaving reaction with tetrazine. We have utilized this switchable fluorescence event for studying the Dox release under different times points, tetrazine concentrations and pH. In order to study the Dox release from a solid surface a doxorubicin nanodrug was assembled using clinically assessed iron oxide nanoparticle (NPs)[13] and Dox-TCO-NHS. The release of Dox was observed from the nanodrug assembly with various tetrazine administrations and time points. Dox release studies were also carried out in metastatic MDA-MB-231 breast cancer cells. Increase in Dox signal was observed upon tetrazine administration indicative of Dox release in the cellular environment. This switchable fluorescence mechanism of Dox could be employed for fundamental studies, i.e., the reactivity of various tetrazine and TCO linker types under different experimental conditions though bond-breaking bioorthogonal reaction. In addition, the system could be instrumental for

translational research where the release and activation of doxorubicin pro-drug payloads can be monitored by optical imaging systems in a label-free fashion.

Experimental Section

Materials

Doxorubicin (Dox) was purchased from LC Laboratories (Woburn, MA) and functionalized with NHS-TCO-NHS linker as described below. Dox and Dox-TCO-NHS were resuspended in phosphate buffer solution (PBS, 100 mM sodium phosphate, 150 mM NaCl, pH 7.2, working buffer) for the bioconjugation studies. Tetrazine was synthesized according to previous reports.[4c, 14] The nanoparticles (NPs) with an average particle size of 32 nm were synthesized according to our previous reports[15] and the brief procedure described below. The modified NPs were purified using Sephadex PD-10 columns purchased from GE Healthcare (Troy, NY). Dulbecco's Modified Eagles Medium (DMEM) was purchased from Corning Life Sciences (CellGro, Corning, NY) and supplemented with Fetal Bovine Serum (FBS, Gibco, Thermo Fischer Scientific, Waltham, MA) and streptomycin/penicillin (Life Tech Corp., Grand Island, NY). Cy5.5-mono NHS ester was purchased from GE Healthcare and attached to the nanoparticles as described below.

Methods

Nanoparticle Synthesis. The superparamagnetic iron oxide nanoparticles (NPs) were synthesized according to literature reports.[15] First, 18 g of Dextran-T10 (Pharmacosmos, Holbaek, Denmark) was mixed with 60 mL of double-distilled water. The resulting suspension was stirred and dissolved completely in a round bottom flask in an ice bath. 1.3 g of $FeCl_3.6H_2O$ (Sigma Aldrich) was added into the clear dextran suspension while flushing Nitrogen gas into the reaction mixture. 0.8 g of $FeCl_2{\cdot}4H_2O$ (Sigma Aldrich) was dissolved in 5 mL of distilled water and immediately added into the reaction mixture. To avoid oxidation of Fe^{2+} this step was done promptly using a distilled water flushed with Nitrogen gas for 5 min prior to addition. 30 mL of concentrated cold NH_4OH (~28%) was added to the stirring mixture forming a slurry green mixture. The temperature of the mixture was raised to 75-85 °C over ~1 hr and kept at this temperature interval for another hour. The resulting NP mixture was cooled to room temperature and concentrated to 40 mL using Amicon Ultra centrifugal units (MWCO 100 kDa; Millipore, Billerica, MA, USA).

In order to crosslink the dextran coating of the NPs, 70 mL of concentrated NaOH (5 M) and 20 mL of concentrated epichlorohydrin (Sigma-Aldrich) was added to the mixture and stirred at least for 8 hr. The NPs were aminated by the addition of 120 mL of NH_4OH (~28%, Sigma-Aldrich) and stirred for an additional 24 hr. The aminated dextran coated NPs were purified using a dialysis bag (MWCO 14 kDa, SpectrumLabs, Dominguez, CA) against distilled water. The NPs were resuspended in working PBS buffer (pH 7.2) for future studies. The concentration of NPs was determined using Cary 60 UV-vis spectrophotometer (Agilent Technologies, Inc., USA) and adjusted to be ~17.0 mg Fe/mL (~38 μM). The number of amine (NH_2) per NP was determined to be ~200 according to SPDP conjugation method described in our previous reports.[2b, 4c, 15-16]

***Trans*-Cyclooctene (TCO) Synthesis and Chemical Conjugation.** The NHS-TCO-NHS was synthesized according to the procedure described in the literature.[17] *Synthesis of Dox-TCO-NHS:* NHS-TCO-NHS (1.75 g, 4.14 mmol, 1.2 equivalent) was added in to a solution of Doxorubicin-HCl (2 g, 3.45 mmol, 1 equivalent) and *N*,*N*-Diisopropylethylamine (DIPEA, 1.34 g, 10.35 mmol, 3 equivalent) in 75 mL of Dimethylformamide (DMF), **Scheme S1**. The resulting mixture was allowed to stir for 12 hr and quenched with 150 mL water. The mixture was extracted with EtOAc (3 x 200 mL) and the combined organic phases were washed with brine and dried over Na_2SO_4. After removal of the solvent, the residue was purified on Biotage (5% MeOH in Dichloromethane) to yield Dox-TCO-NHS (2.16 g, 73%).

^{1}H NMR ($CDCl_3$, 400 MHz) δ: 13.92 (d, 2H), 13.18 (d, 2H), 8.01 (d, *J* = 7.7 *Hz*, 1H), 7.75 (q, *J* = 8.8 *Hz*, 1H), 7.36 (t, *J* = 8.2 *Hz*, 1H), 5.97 (m, 1H), 5.61 (m, 1H), 5.51 (s, 1H), 5.31 (d, , *J* = 2.6, 1H), 5.22 (s, 1H), 5.12 (s, 1H), 4.76 (m, 2H), 4.12 (d, *J* = 5.3, 1H), 4.03 (d, *J* = 6.4, 3H), 3.89 (m, 1H), 3.70 (m, 1H), 3.25 (m, 1H), 2.79 (s, 4H), 2.34−1.74 (broad, m, 14H), 1.31 (d, *J* = 4.1, 3H) , 1.21 (s, 2H) , 1.17 (s, 3H).

HRMS (ESI): calcd. for $C_{42}H_{46}N_2O_{17}Na$ $[M+Na]^+$ m/z 873.2689; found 873.2694.

Synthesis of Tetrazine: Isobutyronitrile (10 mmol) and zinc triflate (0.5 mmol) were mixed with anhydrous hydrazine (1.6 mL). The resulting mixture was stirred for 24 hr at 60 °C under Nitrogen flow and diluted with DMF (2 mL). An aqueous solution of $NaNO_2$ (3.5 g in 50 mL) was slowly added to the mixture. Later, 2M aqueous HCl was added slowly to the mixture until the final acidity was brought to pH 3. The last step generates highly toxic fumes, containing reactive nitrogen species thus extreme caution should be taken. CH_2Cl_2 (3x100 mL) was used to extract the product which was dried with Na_2SO_4. The final product was obtained by chromatography using 1% Et_2O in pentane (1.2 g, 72%).[4b]

^{1}H NMR ($CDCl_3$, 400 MHz) δ: 3.62 (sep, *J* = 6.8 *Hz*, 2H), 1.51 (d, *J* = 6.9 *Hz*, 12H).

^{13}C NMR ($CDCl_3$, 100 MHz) δ: 173.69, 34.14, 21.22.

HRMS (DART) *m/z*: calcd. for $C_8H_{15}N_4$ $[M+1]^+$ 167.1297; found 167.1306.

Molar Absorption Coefficient of Dox-TCO-NHS: 150 μM of aqueous solution of Dox-TCO-NHS (MWT: 850 g/mol) was prepared by dissolving 10 mg in working PBS buffer. Various concentrations (150, 75, 37.5, 18.8 and 9.4 μM) of Dox-TCO-NHS were prepared by serial dilution of the stock solution. Absorbance spectra and endpoints at 493 nm were obtained using Cary 60 UV-vis spectrophotometer (Agilent Technologies, Inc., USA). The maximum absorbance at 493 nm of each sample vs. concentration was plotted and the slope of the linear curve was used to determine the molar absorption coefficient (ε) which was found to be 7747 $M^{-1}cm^{-1}$, **Fig S3**. Absorbance spectra of 50 μM Dox and Dox-TCO-NHS were recorded using a Cary 60 UV-vis spectrophotometer, **Fig 1a**. The absorbance spectra of 50 nM Dox-TCO-NP and NP were collected to calculate number of Dox and cy5.5 per NP, **Fig 3b**.

Nanoparticle Functionalization: Dox-TCO-NP were prepared by addition of freshly prepared Dox-TCO-NHS (40 μL of 25 mM, 100 equivalents) and cy5.5-NHS (5 μL of 10 mM, 5 equivalents) in 250 μL of stock NPs (17.0 mg Fe/mL, 38 μM) in working PBS (pH 7.2) buffer. The mixture was incubated in the dark for 24 hr at room temperature and later purified using Sephadex PD-10 columns against PBS buffer pH (7.2). The NP band in the column was collected whereas free unconjugated molecules and byproducts were discarded. The number of cy5.5 and Dox-TCO per NP was calculated by reading the maximum absorbance of Dox-TCO-NHS (ε_{493}=7747 $M^{-1}cm^{-1}$) and cy5.5 (ε_{675}=250,000 $M^{-1}cm^{-1}$). The absorbance of unmodified NPs was subtracted from that of Dox-TCO-NP. The number of Dox-TCO and cy5.5 was found to be 75 Dox-TCO/NP and 2.5 cy5.5/NP, respectively, **Fig 3b**.

Tetrazine induced doxorubicin release kinetics: 150 μL of 10 μM Dox-TCO-NHS in 100 mM PBS (pH 7.2) buffer was treated with 10 μM, 20 μM, 40 μM, 100 μM and 500 μM (1, 2, 4, 10 and 50 folds) tetrazine prepared from 1.5 mM of stock tetrazine solution. The fluorescence was measured over 4 hr using a BioTek Synergy H1 or a Fluorolog3 spectrofluorometer (λ_{ex} = 493 nm, λ_{em} = 595 nm), **Fig 2b**. The tetrazine-triggered Dox release from NPs was studied in similar manner using 150 μL of 150 nM Dox-TCO-NP (equivalent to ~10 μM Dox-TCO). The emission at 595 nm was

measured (λ_{ex} = 493 nm) to study the release kinetics of Dox and emission at 700 nm was measured for cy5.5 fluorescence (λ_{ex} = 670 nm) as an internal reference **Fig 3c-d**. f/f_0 (final fluorescence/initial fluorescence) ratios were calculated and plotted for Dox and Cy5.5. The kinetic runs were repeated in DMSO in a similar manner to study the mechanism of quenching. In order to study the pH dependence, the experiments were performed using 100 µM Dox-TCO-NHS in pH 4, pH 5 and pH 6, (citrate, 100 mM), pH 7 and pH 8 (PBS, 100 mM) buffers with/without 4 hr post-tetrazine (1 mM) administration, **Fig S5**.

For fluorescent images 150 µL of 10 µM Dox-TCO-NP mixed with 10 µM, 20 µM, 40 µM, 100 µM and 500 µM (1, 2, 4, 10 and 50 folds) for 4 hr, **Fig 4c**. Fluorescent images of MNP-Dox-TCO were taken using a Bio-Rad ChemiDoc system. Fluorescence spectra of the resulting mixtures were recorded using a Fluorolog3 spectrofluorometer (λ_{ex} = 484 nm)**, Fig 2a**.

Cell Culture: The MDA-MB-231 line was obtained from the American Type Culture Collection (ATCC). The cell line was cultured in Dulbecco's Modified Eagles Medium (DMEM). Growth media for each line was supplemented with 10% fetal bovine serum (FBS) and 1% penicillin/streptomycin. All cells were cultured at 37 °C in a humidified incubator supplied with 5% CO_2 according to suppliers' instructions.

Cellular Uptake of the conjugated MNPs: ~50,000 cells were plated on MatTek glass bottom plates for 24 hr for confocal microscopy imaging. The cells were then treated with ~150 nM (67 µg Fe/mL) Dox-TCO-NP and incubated for another 24 hr. On the third day, the medium was removed, and the cells were treated with 10 µM (1 µL of a 1 mM stock) of tetrazine in 1.5 mL of fresh DMEM and incubated for additional 24 hr. Controls were performed in the absence of tetrazine addition. On the final day, the cells were washed, and the medium was replaced with fresh DMEM 4 hr prior to confocal microscopy studies. The confocal images were collected at green and red channels to reconstruct fluorescent images of cells.

For flow cytometry analysis, the cells were cultured according to the aforementioned confocal studies. However, the cells were fixed immediately after the 24 hr incubation with tetrazine. Briefly, the cells were washed twice with PBS and then detached using trypsin 24 hr after tetrazine addition. The cells were resuspended in 4% paraformaldehyde in PBS and kept at 4 °C for 15 minutes. The cells were washed with 2% FBS in PBS twice and then resuspended in 1.5 mL of the same 2% FBS in PBS solution. Data was acquired using a FACS Aria III cell sorter equipped with a 488 nm/Blue Coherent Sapphire solid-state laser, 20 mW (BD Biosciences, San Jose, CA, USA) and analysed using FlowJo software (Ashland, OR, USA), according to the manufacturer's instructions.

Equipment Usage and Data Analysis: A Zeiss LSM 710 Pascal laser confocal microscope (Carl Zeiss Microscopy, Thornwood, NY, USA) was used for fluorescence microscopy images which were analyzed using the Zeiss ZEN 2012 Confocal Microscopy Software.

Bio-Rad ChemiDoc was used to record fluorescent images of Dox-TCO-NP and Dox-TCO in plate readers. Absorbance spectra were collected using a Cary 60 UV-vis spectrophotometer (Agilent Technologies, Inc., USA). Fluorescence recovery kinetics were recoded using a BioTek Synergy H1 or a Fluorolog3 spectrofluorometer and spectra were collected using a Fluorolog3 spectrofluorometer. BD FACS Aria III sorter was used for FACS studies.

Author contributions. MY and MR conceived the study. MY, MR and TBU designed the experiments. TBU performed all the nanoprobe synthesis, characterization and *in vitro* experiments. KW synthesized the chemically modified Dox molecules. IK and MH helped with FACS and *in vitro* analysis, respectively. MY, MR and TBU wrote the manuscript.

Supporting Information. The results of additional experiments, reactions schemes and characterizations are provided in the supplementary document.

Acknowledgements

This work is supported by National Institute of Health (NIH) 1R15GM12811501.

Keywords: doxorubicin • nanoparticle • bioorthogonal chemistry • bond-cleaving • fluorescence imaging

[1] a) C. S. Kim, R. Mout, Y. Zhao, Y. C. Yeh, R. Tang, Y. Jeong, B. Duncan, J. A. Hardy, V. M. Rotello, *Bioconjug. Chem.* **2015**, *26*, 950-954; b) R. Tang, Z. Jiang, M. Ray, S. Hou, V. M. Rotello, *Nanoscale* **2016**, *8*, 18038-18041; c) C. M. Alexander, M. M. Maye, J. C. Dabrowiak, *Chem. Commun.* **2011**, *47*, 3418-3420.

[2] a) S. Mitragotri, D. G. Anderson, X. Chen, E. K. Chow, D. Ho, A. V. Kabanov, J. M. Karp, K. Kataoka, C. A. Mirkin, S. H. Petrosko, J. Shi, M. M. Stevens, S. Sun, S. Teoh, S. S. Venkatraman, Y. Xia, S. Wang, Z. Gu, C. Xu, *ACS Nano* **2015**, *9*, 6644-6654; b) B. Yoo, S. K. Ghosh, M. Kumar, A. Moore, M. V. Yigit, Z. Medarova, *J. Biomed. Nanotechnol.* **2014**, *10*, 1114-1122; c) C. M. Alexander, J. C. Dabrowiak, M. M. Maye, *Bioconjug. Chem.* **2012**, *23*, 2061-2070; d) E. Crew, M. A. Tessel, S. Rahman, A. Razzak-Jaffar, D. Mott, M. Kamundi, G. Yu, N. Tchah, J. Lee, M. Bellavia, C. J. Zhong, *Anal. Chem.* **2012**, *84*, 26-29; e) J. H. Lee, M. V. Yigit, D. Mazumdar, Y. Lu, *Adv. Drug Deliv. Rev.* **2010**, *62*, 592-605.

[3] a) D. Luo, K. A. Carter, J. F. Lovell, *Wiley Interdiscip. Rev. Nanomed. Nanobiotechnol.* **2015**, *7*, 169-188; b) M. S. Shim, Y. J. Kwon, *Bioconjug. Chem.* **2009**, *20*, 488-499; c) R. Tong, R. Langer, *Cancer J.* **2015**, *21*, 314-321; d) R. Mo, T. Jiang, R. DiSanto, W. Tai, Z. Gu, *Nat. Commun.* **2014**, *5*, 3364; e) M. W. Tibbitt, J. E. Dahlman, R. Langer, *J. Am. Chem. Soc.* **2016**, *138*, 704-717; f) C. J. Cheng, R. Bahal, I. A. Babar, Z. Pincus, F. Barrera, C. Liu, A. Svoronos, D. T. Braddock, P. M. Glazer, D. M. Engelman, W. M. Saltzman, F. J. Slack, *Nature* **2015**, *518*, 107-110.

[4] a) I. Khan, L. M. Seebald, N. M. Robertson, M. V. Yigit, M. Royzen, *Chem.Sci.* **2017**, *8*, 5705-5712; b) N. M. Robertson, Y. Yang, I. Khan, V. E. LaMantia, M. Royzen, M. V. Yigit, *Nanoscale* **2017**, *9*, 10020-10030; c) I. Khan, P. F. Agris, M. V. Yigit, M. Royzen, *Chem. Commun.* **2016**, *52*, 6174-6177.

[5] C. Tassa, S. Y. Shaw, R. Weissleder, *Acc. Chem. Res.* **2011**, *44*, 842-852.

[6] a) M. V. Yigit, A. Moore, Z. Medarova, *Pharm. Res.* **2012**, *29*, 1180-1188; b) Z. Medarova, W. Pham, C. Farrar, V. Petkova, A. Moore, *Nat. Med.* **2007**, *13*, 372-377; c) D. Mumcuoglu, M. Sardan Ekiz, G. Gunay, T. Tekinay, A. B. Tekinay, M. O. Guler, *ACS Appl. Mater. Interfaces* **2016**, *8*, 11280-11287; d) S. Sulek, B. Mammadov, D. I. Mahcicek, H. Sozeri, E. Atalar, A. B. Tekinay, M. O. Guler, *J. Mater. Chem.* **2011**, *21*, 15157-15162.

[7] R. Bilan, I. Nabiev, A. Sukhanova, *Chembiochem* **2016**, *17*, 2103-2114.

[8] N. S. Motlagh, P. Parvin, F. Ghasemi, F. Atyabi, *Biomed. Opt. Express* **2016**, *7*, 2400-2406.

[9] J. M. Mejia Oneto, I. Khan, L. Seebald, M. Royzen, *ACS Cent. Sci.* **2016**, *2*, 476-482.

[10] J. Qi, X. Hu, X. Dong, Y. Lu, H. Lu, W. Zhao, W. Wu, *Adv. Drug Deliv. Rev.* **2019**, *143*, 206-225.

[11] T. Zhao, H. Zhou, L. Lei, C. Guo, Q. Yang, T. Gong, X. Sun, X. Song, T. Gong, Z. Zhang, *Nanoscale* **2020**.

[12] a) C. M. Alexander, K. L. Hamner, M. M. Maye, J. C. Dabrowiak, *Bioconjugate Chem.* **2014**, *25*, 1261-1271; b) B. Yoo, A. Kavishwar, A. Ross, P. Wang, D. P. Tabassum, K. Polyak, N. Barteneva, V. Petkova, P. Pantazopoulos, A. Tena, A. Moore, Z. Medarova, *Cancer Res.* **2015**, *75*, 4407-4415.

[13] M. G. Harisinghani, J. Barentsz, P. F. Hahn, W. M. Deserno, S. Tabatabaei, C. H. van de Kaa, J. de la Rosette, R. Weissleder, *N. Engl. J. Med.* **2003**, *348*, 2491-2499.

[14] H. Wu, J. Yang, J. Seckute, N. K. Devaraj, *Angew. Chem. Int .Ed. Engl.* **2014**, *53*, 5805-5809.

[15] M. V. Yigit, S. K. Ghosh, M. Kumar, V. Petkova, A. Kavishwar, A. Moore, Z. Medarova, *Oncogene* **2013**, *32*, 1530-1538.

[16] Z. Medarova, M. Balcioglu, M. V. Yigit, *Methods Mol. Biol.* **2016**, *1372*, 163-179.

[17] R. Rossin, S. M. van Duijnhoven, W. Ten Hoeve, H. M. Janssen, L. H. Kleijn, F. J. Hoeben, R. M. Versteegen, M. S. Robillard, *Bioconjug. Chem.* **2016**, *27*, 1697-1706.

Entry for the Table of Contents

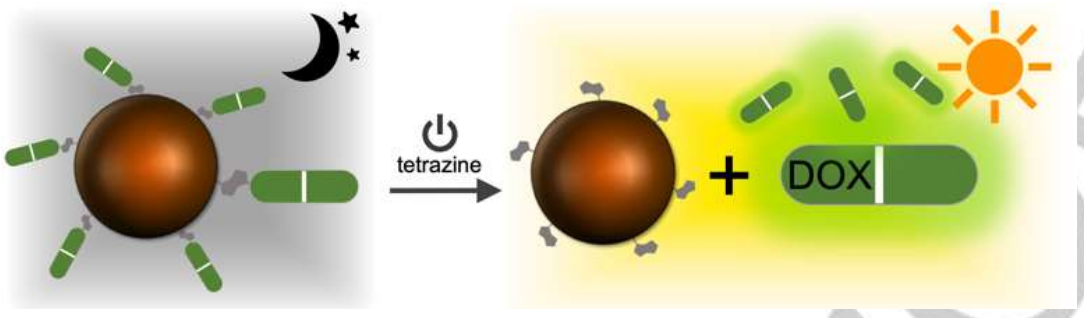

Table of Content Text: The release of a chemotherapeutic drug from a nanodrug formulation is studied using the change in the intrinsic fluorescence of the payload. The release of the doxorubicin with bond-cleaving bioorthogonal reaction is accompanied with doxorubicin's switchable fluorescence property. This fluorescence behavior can validate drug release upon its uncaging reaction with a highly specific chemical partner named "tetrazine". Clinically assessed iron oxide nanoparticles were used to formulate a doxorubicin nanodrug. Increase in doxorubicin fluorescence is exploited to study its release profile from nanoparticle surface upon chemical activation.